November, 1983] © *1983 The Chemical Society of Japan* *Bull. Chem. Soc. Jpn.*, ***56***, *3381—3389 (1983)* 3381

Phosphorescence Studies of $^3\pi\pi^*$ Benzaldehyde, Acetophenone, and 1-Indanone in Benzoic Acid Host

Shin-ichi NAGAOKA and Noboru HIROTA*,†

Department of Chemistry, Faculty of Science, Kyoto University, Sakyo-ku, Kyoto 606

(Received March 26, 1983)

We have made a vibrational analysis of the phosphorescence spectra of benzaldehyde, deuterated benzaldehydes, acetophenone, and 1-Indanone in benzoic acid host. The emissions coming from different sites of benzaldehyde were separated with the help of microwave induced delayed phosphorescence (MIDP) spectroscopy. From the phosphorescence excitation spectra the locations of the $^3n\pi^*$ states were estimated to be about 2000 cm^{-1} above the $^3\pi\pi^*$ states. Contrary to the previous assignment, it was found that the aldehyde H wag is active in the spectra of benzaldehyde as in the cases of other host. The spectra of acetophenone and 1-indanone are similar to those obtained in other hosts, although the 0-0 bands are relatively stronger. The C=O stretching mode is, however, not clearly observable in all the systems studied here, suggesting that this mode is not active in the spectra of nearly pure $^3\pi\pi^*$ aromatic carbonyls. The main radiative mechanisms are discussed based on the present results and are compared with those of other aromatic carbonyls. Possible effects of hydrogen bonding on these properties are discussed.

The lowest excited triplet (T_1) states of aromatic carbonyls of the benzaldehyde type have mixed characters of $^3n\pi^*$ and $^3\pi\pi^*$ states. Their spectroscopic properties are interesting with regard to problems concerning the mixing of two nearby electronic states.[1,2] In recent years there have been considerable efforts to understand the details of the phosphorescence spectra of these molecules.[3-18] In order to fully understand the spectra of carbonyls with mixed characters, it seems desirable to understand first the spectra of pure $^3\pi\pi^*$ carbonyls.

Benzladehyde (abbreviated hereafter as BA) in benzoic acid (abbreviated as BAC), first studied by Koyanagi, Zwarich, and Goodman (KZG),[19] is nearly pure $^3\pi\pi^*$ in character because of the effect of hydrogen bonding. From a vibrational analysis of the phosphorescence spectrum KZG concluded that the aldehyde H wag mode is not active and that the couplings within the singlet manifold are more important than those in the triplet manifold, contrary to the cases of $^3\pi\pi^*$ benzladehydes in other hosts. It has also been a question whether or not the C=O stretching mode is present in the spectra of pure $^3\pi\pi^*$ aromatic carbonyls. Unfortunately the overlapping of the spectra coming from two sites and the presence of a broad background emission prevented KZG from making an unambiguous vibrational analysis. Here we have attempted to separate the emissions of the two sites using microwave induced delayed phosphorescence (MIDP) spectroscopy[20] and reexamined the spectrum of BA in BAC. We have also investigated the phosphorescence spectra of acetophenone (abbreviated as AP) and 1-indanone (abbreviated as 1ID) in BAC in order to see the general characteristics of the phosphorescence spectra of aromatic carbonyls of nearly pure $^3\pi\pi^*$ character.

It has been suggested that the properties of the $^3\pi\pi^*$ aromatic carbonyls of the benzaldehyde type are primarily determined by the energy separations between the $^3n\pi^*$ and $^3\pi\pi^*$ states.[21,22] However, an additional effect due to hydrogen bonding formation might be significant in the present systems. We also examine the magnetic and decay properties of the present systems in connection with those of the related $^3\pi\pi^*$ aromatic carbonyls.

Experimental

Sample Preparation. Commercially obtained BA and AP were purified by repeated distillations under reduced pressure. BA-d_1 (formyl hydrogen deuterated) and BA-d_6 obtained from Merck, Sharp, and Dohme of Canada were used without further purifications. 1ID was purified by recrystallization followed by zone refining. BAC used as host was purified by extensive zone refining. BAC crystals containing small amounts of BA, AP, and 1ID were grown by the Bridgman method. The initial concentrations of the guests in the melts were 2—3 wt%, but the actual concentrations in the crystals are considered to be very low. BAC crystals containing small amounts of anisole were used to obtain the BAC X-trap phosphorescence.

Phosphorescence and MIDP Spectra. The phosphorescence and MIDP spectra were taken at 4.2 K or 1.5 K with a zero field ODMR spectrometer similar to that described in a previous paper.[23] The light from a Xenon arc (XBO 900) or a mercury arc (Osram 500W) was filtered through a water solution saturated with $NiSO_4$ and a Toshiba UV transmitting filter (UVD33S). The phosphorescence emission was dispersed with a Spex 1704 spectrometer (blazed at 300 nm with linear dispersion of 0.83 nm/mm at 428.2 nm) and detected with an EMI 9502 photomultiplier. The phosphorescence intensities given in the tables were corrected for the wavelength dependence of the sensitivity of the detection system by the method given in Ref. 24 with quinine and 2-naphthol. In order to avoid the effect of polarization samples composed of small pieces were used to take the phosphorescence spectra. The polarization behavior of the emission was examined by observing the intensity variation of the phosphorescence with rotation of a polarizing sheet placed parallel to the ab plane of BAC crystal.

In the MIDP experiments microwaves generated by a HP 8900 series tunable microwave oscillator and amplified with a Hughes 1177H microwave amplifier were fed to the sample contained in a helix. In order to separate the spectra coming from the different sites microwave power corresponding to the transition frequency between the sublevels of one site was applied to produce MIDP signal. The

---

[†] Also at the Department of Chemistry, State University of New York at Stony Brook, N.Y. 11794.

MIDP signals generated at the rate of 0.5 Hz were lock-in detected with a PAR 128A lock-in amplifier, while the Spex spectrometer was scanned at the rate of 0.01 nm/s.

In order to take the phosphorescence excitation spectra the light from a 900 W Xenon arc was monochromatized by the Spex spectrometer and focused on the sample of the size of about $10\times5\times4$ mm which was immersed in liquid helium. The entire phosphorescence emission was monitored without using a monochromator.

Results and Discussion

Phosphorescence Excitation Spectra and the Locations of the $^1n\pi^*$ *and* $^3n\pi^*$ *States.* The phosphorescence excitation spectra of BA-d_1 in BAC and BAC X-trap obtained at 4.2 K are shown in Fig. 1. The triplet states of BA and AP in BAC host are generated by the direct absorption of the guests and the absorption of the host followed by the energy transfer to the guests.[25] Comparing the spectra of BAC containing BA or AP with that of BAC X-trap, we can assign the origins of the $S_1\leftarrow S_0$ and $S_2\leftarrow S_0$ transitions. The S_1 and S_2 states are considered to be $^1n\pi^*$ and $^1\pi\pi^*$ (^1L_b) states, respectively. The $T_2\leftarrow S_0$ ($^3n\pi^*$) transitions of the guests were not detected, presumably because the concentrations of the guests were very low. From the peak positions of the a_1 and b bands in Fig. 1 the origins of the $^1n\pi^*$ and $^1\pi\pi^*$ (^1L_b) states of BA-d_1 in BAC were located at 29500 and 32900 cm^{-1}, respectively. The $^1n\pi^*$ state is about 2700 cm^{-1} blue shifted compared with that in methylcyclohexane,[26] whereas the $^1\pi\pi^*$ (^1L_b) state is red shifted by 1500 cm^{-1}. The band a_2 is separated from the band a_1 by 1314 cm^{-1} and is assigned to the vibronic band associated with the C=O stretching vibration in the $^1n\pi^*$ state as in vapor and other hosts.[26] In taking the excitation spectrum of BA, emissions from the different sites were not distinguished. Therefore, the estimated energy separation has an ambiguity of about 200 cm^{-1}. Similarly, the energies of the $^1n\pi^*$ and $^1\pi\pi^*$ (^1L_b) states of AP in BAC were determined to be 29500 and 34000 cm^{-1}, respectively. The energy separations (ΔE_{TT}) between the $^3n\pi^*$ and $^3\pi\pi^*$ of the guests could not be determined directly from the present experiments, but approximate values may be obtained by noting that in the aromatic carbonyls of the benzaldehyde type the energy separations between the $^1n\pi^*$ and $^3n\pi^*$ states are about 1750 cm^{-1}.[21,27] ΔE_{TT} are then estimated using the $^3\pi\pi^*$ energies from the phosphorescence to be 2300 cm^{-1} for BA and 1750 cm^{-1} for AP. These values are much larger than those found for BA and AP in other systems.[26,28,29] This is presumably because hydrogen bonding increases the $^3n\pi^*$ and $^1n\pi^*$ energies. A smaller value of ΔE_{TT} and ΔE_{ST} (energy difference between $^1n\pi^*$ and $^3\pi\pi^*$ states) for AP than for BA probably indicates a weaker hydrogen bonding in AP.

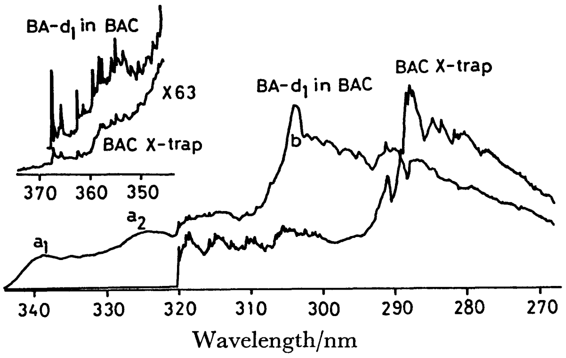

Fig. 1. Phosphorescence excitation spectra of BA-d_1 in BAC and BAC X-trap. The spectra shown in the upper left hand corner show the $T_1\leftarrow S_0$ absorption of BAC host.

Phosphorescence and ODMR Studies. The phosphorescence spectra of BA in the BAC host obtained at 4.2 K are shown in Fig. 2. In these spectra o and o′ peaks are the origins of the emissions coming from two sites as first suggested by Koyanagi *et al.* (KZG).[19] We designate the main vibronic bands using the notations adopted by KZG as much as possible. The phosphorescence spectrum of BA-d_6 in BAC reported by KZG has a broad background emission, but this emission could be eliminated easily by growing the crystals slowly from the melts.[30] It was found that the AP and 1ID spectra consist of the emissions from only one site (Fig. 3).

The o peak gives the ODMR signals at 4.35 and 0.48 GHz; the o′ peak at 4.23, 3.87, and 0.36 GHz in the case of BA-d_1. Deuteration effects on the ODMR frequencies are less than 0.06 GHz. In Table 1 we summarize the results of the ODMR study obtained at 1.5 K. The order of the sublevels is taken to be *z*, *y*, and *x* from the top.[22] It is notable that the energy separations between the *z* and *y* sublevels are very small. This situation is similar to that found

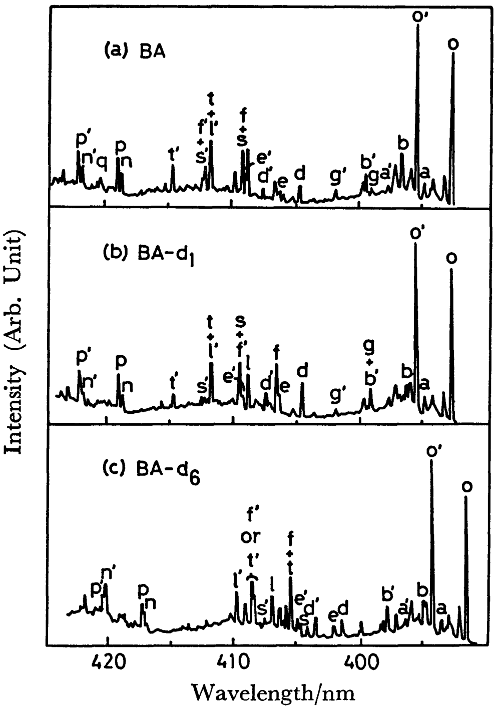

Fig. 2. Phosphorescence spectra of (a) BA, (b) BA-d_1, and (c) BA-d_6 in BAC. The spectra were taken with the slit width of 0.1 mm. No corrections for the peak intensities are made.

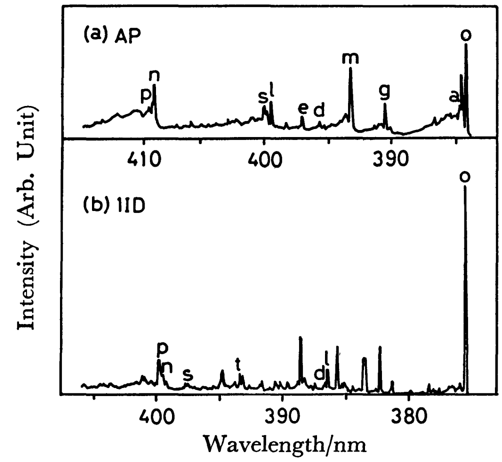

Fig. 3. Phosphorescence spectra of AP and 1ID in BAC. The spectra were taken with the slit width of 0.1 mm. No corrections for the peak intensities are made.

Table 1. ZFS and decay rates of BA-d_1, AP, and 1ID in BAC

	BA-d_1		AP	1ID
	site 1	site 2		
$(Z-X)$/GHz	4.35	4.23	4.66	3.88
$(Z-Y)$/GHz	0.48	0.36	0.72	0.67
$(Y-X)$/GHz	—	3.87	—	—
D/cm^{-1}	−0.0805	−0.0765	−0.0897	−0.0758
E/cm^{-1}	0.0645	0.0645	0.0657	0.0535
k_z/s^{-1}	7.7	6.3	12	14
k_y/s^{-1}	0.33	4.9	1.1	0.53
k_x/s^{-1}	0.32	0.49	0.28	0.27
k_z^r/s^{-1}	1	1	1	—
k_y^r/s^{-1}	0.06	0.71	0.05	—
k_x^r/s^{-1}	0.03	0.06	≈0.02	—
T_1/cm^{-1}	25451	25276	26029	26615
S_1/cm^{-1}	29500		29500	—
S_2/cm^{-1}	32900		34000	—
ΔE_{ST}/cm^{-1}	4050		3500	—
ΔE_{TT}/cm^{-1}	2300		1750	—

for AP in ethylene glycol water studied by Lamola.[31] In spite of the poor molecular symmetry the radiative and total decays of the site 1 BA, AP, and 1ID take place almost exclusively from the z sublevels. The EPR study showed that the z axis is along the C=O direction in the site 1 BA.[32] The x axis is perpendicular to the molecular plane. This is also considered to be true in the cases of AP and 1ID. On the other hand, the EPR study showed that as expected from the decay characteristics the z axis deviates from the C=O direction by 45° in the case of site 2 BA.[32]

We obtained the MIDP spectrum of the z sublevel for the site 1 and those of the z and y sublevels for the site 2 at 1.5 K. The representative spectra are shown in Fig. 4. It was not possible to separate the two emissions completely, but the contribution of the undesired emission was less than 20% of the desired one. We could easily identify the main vibrational bands of the emissions coming from the different sites. In Table 2 we give the results of our vibrational analysis. The analysis was made by comparison with the ground state vibrational frequencies given by Goodman *et al.*[33] The phosphorescence spectra of the site 1 and site 2 are slightly different from each other, but the difference is not large. Our assignments are mostly in agreement with those by KZG, but there are some important difference which are explained in the following.

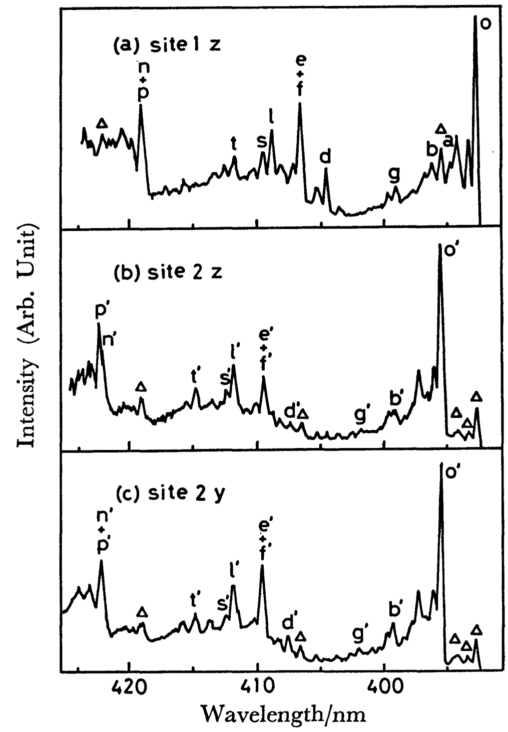

Fig. 4. MIDP specra of BA-d_1 in BAC. All spectra were taken with the slit width of 0.4 mm. The relative intensities of the peaks may not be accurate because of the use of long time constant. The peaks indicated with △ are due to the other site. (a) z sublevel spectrum of the site 1. (b) z subleved spectrum of the site 2. (c) y sublevel spectrum of the site 2.

The main difference is concerned with the assignments of the aldyhyde H wag (f) and ν_{19a} (s). KZG considered that the 0-1024 band (f) in the BA spectrum is due to the ν_{19a} vibration and the aldehyde H wag is not active. We think that this band is mainly due to the aldehyde H wag with a minor contribution from the ν_{19a} vibration, because we observe strong bands at 0-865 (f) and 0-870 (f+t) in the BA-d_1 and BA-d_6 spectra, which can be assigned to the aldehyde D wag. These vibrations are also very active in the site 2 spectra. In the MIDP spectra of BA-d_1 the band due to the ν_{19a} vibration is observable, but the intensity of this band is much weaker than that of the aldehyde D wag. This assignment is further supported by the observation that the polarization behavior of the 0-1024 band is similar to those of the other a'' bands such as CHO wag (b) and is different from those of the 0-0 and other a' bands.[34] Among the a'' bands ν_{16b} and ν_4 vibrations seems to be less active than indicated by KZG.

TABLE 2. VIBRATIONAL ANALYSIS

Band number	Wave number$^{a)}$/cm^{-1}	Relative intensity$^{b)}$	$\Delta\tilde{\nu}$/cm^{-1}	Assignment	Designation
BA site 1$^{c)}$					
0	25456	100	0	0-0 of $^3\pi\pi^*$-$^1A_1$	o
1	25417	20	39	0-39; lattice mode	
2	25359	15	97	0-97; lattice mode	
3	25348	7	108	0-108; lattice mode	
4	25316	13	140	0-140; a″ CHO torsion?	a
7	25202	25	254	0-254; a″ CHO wag	b
11	25096	3	360		
12	25049	5	407	0-407; a″ ν_{16a}	g
15	25009	7	447		
18	24705	13	751	0-751; a″ ν_{11}	d
19	24669	5	787		
21	24607	7	849	0-849; a″ ν_{10a}	e
22	24585	15	871		
24	24458	24	998	0-998; a′ ν_1	l
26	24435	32	1021	0-1021; a″ H wag and a′ ν_{19a}	f+s
28	24284	39	1172	0-1172; a′ ν_{9b}	t
30	24246	11	1210	0-1172-39?	
33	23872	20	1584	0-1584; a′ ν_{8b}	n
34	23857	28	1599	0-1599; a′ ν_{8a}	p
35	23776	8	1680		q
38	23607	13	1849		
BA site 2$^{c)}$					
5	25281	118	0	0-0 of $^3\pi\pi$-$^1A_1$	o′
6	25247	15	34	0-34; lattice mode	
8	25187	5	94	0-94; lattice mode	
9	25168	16	113	0-113; lattice mode	
10	25131	7	150	0-150; a″ CHO torsion	a′
14	25024	12	257	0-257; a″ CHO wag	b′
17	24874	5	407	0-407; a″ ν_{16a}	g′
23	24527	8	754	0-754; a″ ν_{11}	d′
25	24451	10	830	0-830; a″ ν_{10a}?	e′
27	24395	17	886		
28	24284	39	997	0-997; a′ ν_1	l′
29	24256	17	1025	0-1025; a″ H wag and a′ ν_{19a}	f′+s′
31	24106	23	1175	0-1175; a′ ν_{9b}	t′
32	24066	8	1215	0-1175-34?	
36	23697	15	1584	0-1584; a′ ν_{8b}	n′
37	23683	27	1598	0-1598; a′ ν_{8a}	p′
40	23565	4	1716		
BA-d_1 site 1$^{d)}$					
0	25451	100	0	0-0 of $^3\pi\pi^*$-$^1A_1$	o
1	25410	20	41	0-41; lattice mode	
2	25354	13	97	0-97; lattice mode	
3	25344	5	107	0-107; lattice mode	
4	25314	12	137	0-137; a″ CDO torsion	a
7	25221	11	230	0-230; a″ CDO wag	b
9	25186	5	265	0-230-41?	
12	25043	14	408	0-408; a″ ν_{16a}	g
14	25008	10	443	0-408-41?	
16	24762	4	689		
17	24709	25	742	0-742; a″ ν_{11}	d
18	24660	6	791		
19	24598	13	853	0-853; a″ ν_{10a}	e
20	24586	37	865	0-865; a″ D wag	f
21	24550	5	901		

TABLE 2. (Continued)

Band number	Wave number[a)]/cm^{-1}	Relative intensity[b)]	$\Delta\tilde{\nu}$/cm^{-1}	Assignment	Designation
24	24450	27	1001	0-1001; a′ ν_1	l
26	24409	33	1042	0-1042; a′ ν_{19a}	s
27	24277	30	1174	0-1174; a′ ν_{9b}	t
34	23954	4	1497		
35	23867	14	1584	0-1584; a′ ν_{8b}	n
36	23850	32	1601	0-1601; a′ ν_{8a}	p
37	23857	4	1645		
39	23767	4	1684		
40	23752	4	1699		
		BA-d_1 site 2[d)]			
5	25276	114	0	0-0 of $^3\pi\pi^*$-$^1A_1$	o′
6	25243	15	33	0-33; lattice mode	
8	25203	5	73	0-73; lattice mode	
10	25116	15	110	0-110; lattice mode	
12	25043	14	233	0-233; a″ CDO wag	b′
14	25008	10	268	0-233-33?	
15	24869	5	407	0-407; a″ ν_{16a}	g′
22	24532	13	744	0-744; a″ ν_{11}	d′
25	24423	10	853	0-853; a″ ν_{10a}	e′
26	24409	33	867	0-867; a″ D wag	f′
27	24277	30	999	0-999; a′ ν_1	l′
29	24236	6	1040	0-1040; a′ ν_{19a}	s′
31	24098	12	1178	0-1178; a′ ν_{9b}	t′
42	23688	11	1588	0-1588; a′ ν_{8b}	n′
43	23674	27	1602	0-1602; a′ ν_{8a}	p′
44	23623	13	1653		
		BA-d_6 site 1[e)]			
0	25523	100	0	0-0 of $^3\pi\pi^*$-$^1A_1$	o
1	25485	20	38	0-38; lattice mode	
2	25425	12	98	0-98; lattice mode	
3	25412	3	111	0-111; lattice mode	
4	25392	10	131	0-131; a″ CDO torsion	a
7	25306	18	217	0-217; a″ CDO wag	b
8	25277	7	246	0-217-38?	
11	25164	12	359		
17	24901	13	622	0-622; a″ ν_{11}	d
18	24859	9	664	0-664; a″ ν_{10a}	e
20	24772	18	751	0-751; a″ ν_{17b}	
23	24698	10	825	0-825; a′ ν_{19a}	s
25	24651	42	872	0-872; a′ ν_{9b} and/or a″ D wag	t+f
26	24633	17	890		
27	24613	8	910		
29	24563	23	960	0-960; a′ ν_1	l
33	24437	18	1086	0-1050-38?	
39	23964	12	1559	0-1559; a′ ν_{8b}	n
40	23955	21	1568	0-1568; a′ ν_{8a}	p
43	23874	6	1649		
44	23862	6	1661		
45	23851	6	1672		
		BA-d_6 site 2[e)]			
5	25349	120	0	0-0 of $^3\pi\pi^*$-$^1A_1$	o′
6	25316	16	33	0-33; lattice mode	
9	25240	17	109	0-109; lattice mode	
10	25208	7	141	0-141; a″ CDO torsion	a′
12	25122	16	227	0-227; a″ CDO wag	b′
13	25101	7	248	0-227-33?	

TABLE 2. (Continued)

Band number	Wave number[a]/cm^{-1}	Relative intensity[b]	$\Delta\bar{\nu}$/cm^{-1}	Assignment	Designation
14	25088	6	261		
15	24993	11	356		
22	24724	10	622	0-622; a″ ν_{11}	d′
24	24684	12	665	0-665; a″ ν_{10a}	e′
28	24596	16	753	0-753; a″ ν_{17b}?	
30	24522	8	827	0-827; a′ ν_{19a}	s′
31	24479	23	870	0-870; a′ ν_{9b} and/or a″ D wag	t′ or f′
32	24473	34	876	0-876; a′ ν_{9b} and/or a″ D wag	t′ or f′
33	24437	18	912		
34	24396	24	953	0-953; a′ ν_1	l′
35	24364	7	985	0-953-33?	
46	23792	26	1557	0-1557; a′ ν_{8b}	n′
47	23785	13	1564	0-1564; a′ ν_{8a}	p′
48	23699	17	1650		
		AP			
0	26029	100	0	0-0 of $^3\pi\pi^*$-$^1A_1$	o
1	26007	58	22	0-22; lattice mode	
2	25990	14	39	0-39; a″ $COCH_3$ torsion	a
3	25972	7	57		
4	25959	3	70		
5	25937	6	92		
6	25890	6	139	0-139; a″ CH_3 torsion	
7	25855	8	174		
8	25627	7	402		
9	25608	33	421	0-421; a″ ν_{16a}	
10	25584	4	445	0-421-22?	
11	25575	4	454		
12	25549	3	480	0-480; a″ ν_{16b}	
13	25430	70	599	0-599; a′ CCO bend	m
14	25399	10	630	0-599-22?	
15	25286	4	743		
16	25267	8	762	0-762; a″ ν_{11}	d
17	25182	14	847	0-847; a″ ν_{10a}	e
18	25097	7	932	0-932; a″ ν_{17a}	
19	25029	28	1000	0-1000; a′ ν_1	l
20	25005	18	1024	0-1000-22?	
21	24993	21	1036	0-1036; a′ ν_{19a}	s
22	24928	5	1101	0-1101; a′ $\nu(C\text{-}CH_3)$	
23	24856	5	1173	0-1173; a′ ν_{9b}	
24	24812	6	1217		
25	24748	5	1281		
26	24727	3	1302		
27	24684	5	1345		
28	24638	5	1391		
29	24603	8	1426		
30	24575	5	1454		
31	24532	5	1497	0-1497; a′ ν_{18a}	
32	24503	3	1526		
33	24431	55	1598	0-1598; a′ ν_{8b}	n
34	24425	13	1604	0-1604; a′ ν_{8a}	p
35	24402	13	1627	0-1598-22?	
36	24336	10	1693		
37	24251	6	1778		
		IID			
1	26615	100	0	0-0 of $^3\pi\pi^*$-$^1A_1$	o
2	26577	4	38	0-38; lattice mode	

Table 2. (Continued)

Band number	Wave number$^{a)}$/cm^{-1}	Relative intensity$^{b)}$	$\Delta\tilde{\nu}$/cm^{-1}	Assignment	Designation
3	26532	2	83	0-83; lattice mode	
4	26464	2	151		
5	26445	2	170		
6	26431	2	184		
7	26413	5	202		
8	26314	2	301		
9	26215	7	400	0-400; a″ ν_{16b}?	
10	26151	23	464	0-464; a″ γ(C=O)	
11	26125	2	490	0-464-38?	
12	26070	17	545	0-545; a′ ν_{6b}	
13	26065	17	550	0-550; a′ ν_{6a}	
14	26002	2	613	0-613; a′ $\delta(CCC_p)$	
15	25956	4	659		
16	25942	3	673		
17	25920	22	695	0-695; a″ $\nu(CCC_b)$	
18	25871	10	744	0-744; a′ ν_1	l
19	25854	3	761	0-761; a″ ν_{11}	d
20	25798	3	817	0-817; a″ $\gamma(CH_2)$	
21	25777	2	838	0-838; a′ ν_{12}	
22	25745	4	870		
23	25731	24	884	0-884; a″ ν_{10b}	
24	25713	3	902	0-884-38?	
25	25663	3	952	0-952; a′ $\nu(CC_p)$	
26	25620	3	995	0-995; a″ ν_5	
27	25592	3	1023	0-1023; a′ w(CH_2)	
28	25528	5	1087	0-1087; a″ tw(CH_2)	
29	25514	2	1101	0-1101; a′ ν_{18b}	
30	25458	2	1157	0-1157; a′ ν_{15}	
31	25425	7	1190		
32	25410	7	1205	0-1205; a′ ν_{9b}	t
33	25384	4	1231	0-1231; a′ ν_{7b}	
34	25325	9	1290		
35	25148	3	1467	0-1467; a′ ν_{19a}	s
36	25136	3	1479	0-1479; a′ ν_{19b}	
37	25036	4	1579		
38	25018	5	1597	0-1597; a′ ν_{8b}	n
39	25005	12	1610	0-1610; a′ ν_{8a}	p
40	24933	4	1682		
41	24918	4	1697		

a) The wave numbers in this table refer to vacuum. b) The relative intensities in this table are peak ones and their ambiguities are about 5%. c) The following peaks could be assigned to neither site 1 nor site 2. (numbers in the parenthesis are the relative intensities) 25034(2), 25000(4), 24624(6), and 23589(4). d) 25130(7), 25029(3), 24482(7), 24256(4), 24218(7), 24081(4), 24042(8), 23781(4), 23710(6), and 23589(6). e) 24082(4), 24809(4), 24763(4), 24253(6), 24169(5), 23976(7), 23923(6), and 23900(4).

Another important difference exists concerning the estimate of the intensity of the C=O stretching bands. According to the KZG assignment the C=O stretching bands have moderate intensities in the spectra of BA, BA-d_1, and BA-d_6. Although there is a 0-1680 (q) band of moderate intensity in the BA, there is no corresponding band in the BA-d_1 spectrum. Therefore, the C=O stretching band is likely to be very weak in the present systems. The C=O stretching band is also not clearly observable in the AP and 1ID spectra. The vibrations appearing in the AP spectrum are similar to those appearing in the spectra of AP X-trap[35] and AP in AP-d_8[19] except that the C=O stretching band is not clearly observable in AP in BAC. The common features of the spectra of BA and AP in BAC may be summarized as follows.

1) The 0-0 band is very strong.

2) The C=O stretching band is not clearly observable.

3) The main a′ modes associated with the ring vibrations are ν_1 (l), ν_{19a} (s), ν_{9b} (t), ν_{8b} (n), and ν_{8a} (p).

4) In addition to the a″ vibrations associated with the CHO and CH_3CO groups ν_{16a} (g), ν_{11} (d), and ν_{10a} (e) a″ ring modes have moderate intensities.

In connection with the observations recently made about the spectra of benzaldehyde, two points should be noted. One is about the intensity of the C=O stretching band. The C=O stretching vibration has been found widely in the phosphorescence spectra of the $^3\pi\pi^*$ aromatic carbonyls and it was suspected that it may have an intramolecular origin.9) We have previously suggested that the appearance of this mode in the spectra of the $^3\pi\pi^*$ aromatic carbonyls is primarily due to the direct configurational mixing of the nearby $^3n\pi^*$ and $^3\pi\pi^*$ states caused by distortion and that it should not be active in the spectra of the nearly pure $^3\pi\pi^*$ aromatic carbonyls with large ΔE_{TT}.5) The present result supports this suggestion further. Another point of interest is the relative intensities of the H wag and CHO torsion mode.9) It was found that the intensity of the H wag is much stronger than that of the CHO torsion band as in the cases of many other $^3\pi\pi^*$ benzaldehydes.12,25)

The phosphorescence spectrum of 1ID in BAC is also characterized by a very strong 0-0 band and a number of a″ vibronic bands with moderate to weak intensities. The vibrations appearing in the spectrum of 1ID in BAC are similar to those appearing in the 1ID X-trap spectrum,33) but the relative intensity of the 0-0 band is much stronger in the BAC host. We made a vibrational analysis using infrared and Raman data.36)

In the cases of BA, AP, and 1ID in BAC the phosphorescence takes place predominantly from the *z* sublevel. It was previously suggested that the *z* sublevel emissions of the $^3\pi\pi^*$ aromatic carbonyls are mainly due to the following three mechanisms.5) (I) $^3n\pi^*$-$^3\pi\pi^*$ configurational mixing, (II) $^1n\pi^*$-$^3\pi\pi^*$ spin orbit coupling, (III) Herzberg-Teller vibronic spin orbit mechanism. However, the $^3n\pi^*$-$^3\pi\pi^*$ configurational mixing is not important in the present systems possibly because of large ΔE_{TT} and the planar structure of the T_1 states. Then the mechanism to produce the *z* sublevel emission at the 0-0 and the a′ band is,

$$\text{(II)}\quad {}^3\pi\pi^*(z) \xleftrightarrow{\text{S.O.}} {}^1n\pi^* \xleftrightarrow{e\vec{r}} S_0.$$

The Hertzberg-Teller vibronic spin orbit mechanism in both triplet and singlet manifolds gives rise to the a″ bands,

(III)

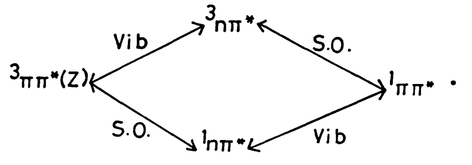

However, in view of the fact that ΔE_{TT} is smaller than the energy separations between the $^1n\pi^*$ and $^1\pi\pi^*$ states vibronic coupling within the triplet manifold is considered to be more important as in the other $^3\pi\pi^*$ benzladehydes.5) The relative importance of the mechanism (III) with respect to that of (II) is reduced as ΔE_{TT} increases. This is the reason why the a″ vibronic bands are relatively weak compared with the 0-0 bands in the present systems. The phosphorescence spectra of the present systems are thus explained by the same radiative mechanisms as used previously to explain the other $^3\pi\pi^*$ aromatic carbonyls. It should be noted that the present mechanisms are essentially the same as those discussed for AP in ethylene glycol water by Lamola.31)

The phosphorescence of the site 2 BA comes from both *z* and *y* sublevels with $k_z^r/k_y^r=0.71$ at the 0-0 band. Our EPR study showed that the z axis of the zero field tensor is 45° away from the C=O direction and this is the cause of the two sublevel activities in the site 2.32) In fact, the *y* sublevel spectrum is quite similar to the *z* sublevel one. If the spin orbit mixing with the $^1n\pi^*$ state is responsible for the emissions from both y and z sublevels, the deviation of the *z* axis from the C=O direction is given by arctan $\sqrt{0.71}=40°$,21) which is in reasonable agreement with the value determined by the EPR study.33)

The EPR study showed that the spin distribution in the benzene ring of the T_1 state of BA in BAC is very similar to that of the T_1 state of benzonitrile. The T_1 states of BA in BAC and benzonitrile have similar quinonoid structures.32,37) Then it may be expected that the modes associated with the benzene ring vibrations appearing in the phosphorescence spectra are similar in both systems. The phosphorescence spectrum of benzonitrile is simple consisting of the bands at 0-765, 0-1000, 0-1185, and 0-1610.38) Indeed these bands have moderate intensities in the spectrum of BA in BAC.

Comparison with the Other $^3\pi\pi^*$ Carbonyls. The spectroscopic properties of BA, AP, and 1ID in BAC are mostly well explained by taking account of the fact that ΔE_{TT} are much larger than those of BA, AP, and 1ID in other hosts. However, there seem to be a few characteristics which are specific to the present systems.

It was shown previously that there is a good empirical correlation between the decay rate constant of the *z* sublevel of a $^3\pi\pi^*$ aromatic carbonyl and ΔE_{TT} or ΔE_{ST}.21,22) This correlation with $\Delta E_{ST}=4050\ \text{cm}^{-1}$ predicts k_z of BA in BAC to be $17.6\ \text{s}^{-1}$, which is in good agreement with the observed $18\ \text{s}^{-1}$.22) For a series of $^3\pi\pi^*$ aromatic carbonyls of the benzaldehyde type it was previously suggested that $k_y^r(0\text{-}0)/k_z^r(0\text{-}0)$ increases as ΔE_{TT} (ΔE_{ST}) increases.5) There are a few carbonyls with large ΔE_{TT} in which $k_y^r(0\text{-}0)$ are even larger than $k_z^r(0\text{-}0)$.39,40) Here, however, $k_y^r(0\text{-}0)/k_z^r(0\text{-}0)$ is very small in spite of rather large ΔE_{TT}. This is probably due to two causes. Firstly, $k_y^r(0\text{-}0)$ is very small. The fact that k_y of the site 1 BA and 1ID are much smaller than those of the other $^3\pi\pi^*$ aromatic carbonyls of the benzaldehyde type seems to indicate this. This shows that the radiative decay involving the spin-orbit mixing with the $^1\sigma\pi^*(^1\pi\sigma^*)$ state is not very effective in the present systems. Secondly, $k_z^r(0\text{-}0)$ is relatively large in the present systems probably because of the increased intensity of the $S_0 \rightarrow S_1(^1n\pi^*)$ transition. Although we do not know the exact reason of the very small $k_y^r(0\text{-}0)/k_z^r(0\text{-}0)$ here, hydrogen bonding formation may be responsible.

The ZFS were determined by using the spin Hamiltonian, $H=-XS_x^2-YS_y^2-ZS_z^2$, with $D=-3/2Z$

and $E=\frac{1}{2}(Y-X)$. X, Y, and Z are the energies of the x, y, and z sublevels, respectively, with $X+Y+Z=0$. $|D|=0.0805\ \mathrm{cm}^{-1}$ for BA-d_1, $0.0897\ \mathrm{cm}^{-1}$ for AP, and $0.0758\ \mathrm{cm}^{-1}$ for 1ID in BAC are rather small compared with those of the other $^3\pi\pi^*$ aromatic carbonyls. D is given as a sum of D_{SO} due to the second order effect of the spin orbit interaction and D_{SS} due to spin-spin interaction. D_{SO} is given approximately as[41,42]

$$D_{\mathrm{SO}} = -G^2(1/\Delta E_{\mathrm{TT}} - 1/\Delta E_{\mathrm{ST}}).$$

Here G is the matrix element for the spin-orbit mixing between $^3n\pi^*$ and $^3\pi\pi^*$ states. G^2 was estimated to be ≈ 90, ≈ 60, and $\approx 20\ \mathrm{cm}^{-2}$ for a series of benzaldehydes, acetophenones, and 1-indanones.[21,22,43] With the values of ΔE_{TT} and ΔE_{ST} estimated in this work, these values give D_{SO} for BA, AP, and 1ID to be -0.017, -0.017, and $-0.006\ \mathrm{cm}^{-1}$, respectively. On the other hand, D_{SS} estimated for a series of benzaldehydes and 1-indanones are $-0.11\ \mathrm{cm}^{-1}$ and $-0.08\ \mathrm{cm}^{-1}$ from plots of D_{obs} *vs.* $1/\Delta E_{\mathrm{TT}} - 1/\Delta E_{\mathrm{ST}}$.[21,22,43] These values predict D to be -0.127 and $-0.086\ \mathrm{cm}^{-1}$, respectively. The observed D are somewhat larger than these estimates. Our previous MO calculation showed that hydrogen bonding caused significant changes in the spin distribution on the carbonyl group.[31] D_{SS} and D_{SO} may be affected significantly through the changes in spin distribution.

We express our sincere thanks to Dr. Motohiko Koyanagi of Kyushu University for his helpful and critical discussions. Our thanks are also due to Dr. Seigo Yamauchi for valuable discussions, Mr. Yoshihiro Hirata for his help in the early stage of this work and Miss Yasuko Yamada for the correction of the wavelength dependence of the spectrometer and the polarization data. This work was partly supported by a Grant from the Ministry of Education, Science and Culture.

References

1) A. J. Duben, L. Goodman, and M. Koyanagi, "Interstate Interaction in Aromatic Aldehydes and Ketons," in "Excited States," ed by E. C. Lim, Academic Press, New York (1974), Vol. 1, pp. 295—329.

2) E. C. Lim, "Vibronic Interactions and Luminescence in Aromatic Molecules with Nonbonding Electrons," in "Excited States," ed by E. C. Lim, Academic Press, New York (1977), Vol. 3, pp. 305—337.

3) W. Moehle and M. Vala, *Chem. Phys. Lett.*, **41**, 149 (1976).

4) A. Despres and E. Migirdicyan, *Chem. Phys.*, **14**, 229 (1976).

5) E. T. Harrigan and N. Hirota, *Mol. Phys.*, **31**, 681 (1976).

6) M. Koyanagi, K. Higashi, and Y. Kanda, *Chem. Phys. Lett.*, **52**, 184 (1977).

7) O. S. Khalil, S. W. Hankin, and L. Goodman, *Chem. Phys. Lett.*, **52**, 187 (1977).

8) I-Fu Hung, D. F. Williams, and R. Yip, *J. Lumin.*, **15**, 231 (1977).

9) I. Özkan and L. Goodman, *Chem. Phys. Lett.*, **64**, 32 (1979).

10) M. Koyanagi and L. Goodman, *Chem. Phys.*, **39**, 237 (1979).

11) I. Özkan and L. Goodman, *Chem. Rev.*, **79**, 275 (1979).

12) A. Despres, V. Legeune, E. Migirdicyan, and W. Siebrand, *Chem. Phys.*, **36**, 41 (1979).

13) L. Goodman, M. Lamotte, and M. Koyanagi, *Chem. Phys.*, **47**, 329 (1980).

14) Y. Hirata and E. C. Lim, *J. Chem. Phys.*, **72**, 5505 (1980).

15) A. Despres and E. Migirdicyan, *Chem. Phys.*, **50**, 381 (1980).

16) J. S. Patel and D. M. Hanson, *Chem. Phys.*, **69**, 249 (1982).

17) I. C. Winkler and D. M. Hanson, *J. Chem. Phys.*, **76**, 5739 (1982).

18) A. Despres, V. Lejeune, and E. Migirdicyan, *Chem. Phys.*, **66**, 57 (1982).

19) M. Koyanagi, R. J. Zwarich, and L. Goodman, *J. Chem. Phys.*, **56**, 3044 (1972).

20) J. Schmidt, W. S. Veeman, and J. H. van der Waals, *Chem. Phys. Lett.*, **4**, 341 (1969); D. A. Antheunis, J. Schmidt, and J. H. van der Waals, *ibid.*, **6**, 255 (1970); *Mol. Phys.*, **22**, 1 (1971).

21) E. T. Harrigan and N. Hirota, *Mol. Phys.*, **31**, 663 (1976).

22) Y. Hirata and N. Hirota, *Mol. Phys.*, **39**, 129 (1980).

23) T. H. Cheng and N. Hirota, *J. Chem. Phys.*, **56**, 5019 (1972).

24) H. Kokubun, "Keiko," in "Shin Zikken Kagaku Koza" ed by the Chemical Society of Japan, Maruzen, Tokyo (1976), Vol. 4, Kiso Gizyutsu 3, Hikari (II), Chap. 8, pp. 505—549.

25) The bands starting at 320 and 292 nm of the excitation spectrum of the BAC trap are due to $T_2(^3n\pi^*)\leftarrow S_0$ and $S_1(^1\pi\pi^*)\leftarrow S_0$ absorptions of BAC, respectively.

26) L. Goodman and M. Koyanagi, *Mol. Photochem.*, **4**, 369 (1972).

27) H. Hayashi and S. Nagakura, *Mol. Phys.*, **27**, 969 (1974).

28) T. H. Cheng and N. Hirota, *Mol. Phys.*, **27**, 281 (1974).

29) W. A. Case and D. R. Kearns, *J. Chem. Phys.*, **52**, 2175 (1970).

30) Dr. M. Koyanagi also made the same observation. Private communication.

31) A. A. Lamola, *J. Chem. Phys.*, **47**, 4810 (1967).

32) S. Nagaoka and N. Hirota, *J. Chem. Phys.*, **74**, 1637 (1981).

33) R. Zwarich, J. Smolarek, and L. Goodman, *J. Mol. Spectrosc.*, **38**, 336 (1971).

34) The following values (numbers given in parenthesis) were obtained for I_b/I_c of the a′ and a″ bands of BA at site 1, respectively. a′ bands; 0-0(2.74), 0-998(1.88) 0-1584 (2.04), 0-1599(2.18), a″ bands; 0-254 (0.68), 0-751 (0.40), 0-1021 (0.81). Private communication from Y. Yamada.

35) S. Niizuma and N. Hirota, *J. Phys., Chem.*, **82**, 453 (1978).

36) L. Bardet, G. Fleury, R. Granger, and C. Sablayrolles, *J. Mol. Struct.*, **3**, 141 (1969).

37) N. Hirota, T. C. Wong, E. T. Harrigan, and K. Nishimoto, *Mol. Phys.*, **29**, 903 (1975).

38) L. Lebel and J. P. Laposa, *J. Mol. Spectrosc.*, **41**, 249 (1972).

39) E. T. Harrigan, A. Chakrabarti, and N. Hirota, *J. Am. Chem. Soc.*, **98**, 3460 (1976).

40) M. Baba, N. Hirota, and E. M. Kosower, *J. Phys. Chem.*, **85**, 1469 (1981).

41) H. Hayashi and S. Nagakura, *Mol. Phys.*, **24**, 801 (1972).

42) C. R. Jones, D. R. Kearns, and A. H. Maki, *J. Chem. Phys.*, **59**, 873 (1973).

43) S. Niizuma and N. Hirota, *J. Phys. Chem.*, **83**, 706 (1979).